CRISPR/Cas9 KOs of p53 and STAT1 in HEK293 cells

Tabitha de Haan

S4119959

Research Project Biomedical Sciences (WBBY902-10)

BMS5 Aging Research ERIBA

Supervisor: Mathilde Broekhuis

Foijer lab *'Genomic Instability in Development and Disease'*

University of Groningen (RUG)

7 June 2022

Abstract

Chromosomal instability is a well-known characteristic of cancer and leads to activation of inflammatory signalling. P53 and STAT1 are genes that play a role in this inflammatory response, while OAS1 and IFIT1 may also be involved. To better understand the underlying molecular mechanism, sgRNAs for these four genes were designed and cloned in vectors, to create CRISPR/Cas9 mediated knockout cells. HEK293 cells were transfected with vectors containing sgRNAs for p53 and STAT1. Western blot showed that STAT1 protein level was not decreased in cells targeted for STAT1 KO. The p53 protein level was slightly reduced in p53 KO targeted cells, while PCR and Sanger sequencing of the p53 gene in these cells showed no mutations in the sgRNA target sequence. We conclude that the CRISPR/Cas9 knockout of p53 and STAT1 in HEK293 cells was presumably unsuccessful.

Introduction

Chromosomal instability (CIN) is a state in which cells suffer from errors in chromosome segregation during mitosis. Frequent consequences of CIN are abnormal chromosome numbers or other structural alterations of chromosomes, which are known as aneuploidy [Schukken & Foijer, 2017]. When chromosomes are not yet properly attached to the mitotic spindle, the spindle assembly checkpoint (SAC) will normally halt mitosis. Therefore, anomalies in SAC lead to CIN and conversely premature chromosome segregation and aberrant chromosome copy numbers [Musacchio, 2015; Chen et al., 2022]. In untransformed cells, CIN can lead to cell cycle arrest and apoptosis in a p53-dependent manner [Kadioglu et al., 2021].

More often, CIN and aneuploidy lead to cell death via activation of the inflammatory response. CIN can lead to micronuclei often containing whole chromosomes in cases of aneuploidy [Schukken & Foijer, 2017; Chen et al., 2022]. These micronuclei tend to rupture during the interphase, thereby releasing chromatin into the cytosol, which is sensed by DNA sensors, like cyclic GMP-AMP synthase (cGAS) [Hatch et al., 2013; Mackenzie et al., 2017]. DNA sensors activate the type I interferon response, which ultimately leads to the production of pro-inflammatory cytokines, immune activation and subsequent killing of the aneuploid cell [Chen et al., 2022; Diamond et al., 2011; Wang et al., 2021]. In contrast, CIN and aneuploidy are hallmarks of cancer, as the vast majority of tumours display an aberrant karyotype [Wang et al., 2021]. Aneuploid cancer cells must have adopted mechanisms to avoid clearance by the immune system. It was hypothesised that the inflammatory response in cancer cells with aneuploidy has been altered [Hong et al., 2022].

As previously stated, cGAS activation leads to an inflammatory response. In the signalling cascade, cGAS activates STING, leading to STAT1 activation, immune recruitment and subsequent clearance of the aneuploid cell (see figure 1) [Mackenzie et al., 2017; Chen et al., 2022]. However, aneuploid cancers in particular were found to inactivate STAT1, and thereby seem to avoid immune recognition [Schubert et al., 2021].

Interestingly, cGAS and STING are seldom inactivated in cancer, which likely means that part of the inflammatory signalling is also necessary for cell survival. Indeed, it was found that STING also leads to activation of the non-canonical NF-kB pathway and subsequent IL6/IL-6R/STAT3 signalling (figure 1) [Hong et al., 2022]. Activation of IL-6/IL-6R/STAT3 is highly dependent on STING signalling, which is the reason why cGAS and STING are hardly ever inactivated in primary tumour cells [Bakhoum et al., 2018; Hong et al., 2022]. Moreover, cancer cells seem to upregulate this non-canonical NF-kB pathway, while downregulating the type I interferon response and the associated STAT1 activation [Bakhoum et al., 2018]. In summary, cGAS/STING signalling leads to STAT1 activation, which promotes cancer cell apoptosis, as well as STAT3 activation, which promotes cancer cell survival. Conversely, cancers with CIN exploit cGAS/STING signalling by inactivating STAT1 and activating the non-canonical NF-kB pathway and STAT3 [Hong et al., 2022; Schubert et al., 2021].

Importantly, how all signalling molecules and pathways interact in inflammatory signalling in cancer cells with CIN, is still unclear [Wang et al., 2021]. As aneuploidy and CIN affect the majority of cancers, new therapy regimens could be beneficial for a large patient group [Duijf et al., 2013; Gordon et al., 2012]. This adds to the importance of elucidating the exact mechanisms by which inflammatory signalling works in cells with CIN.

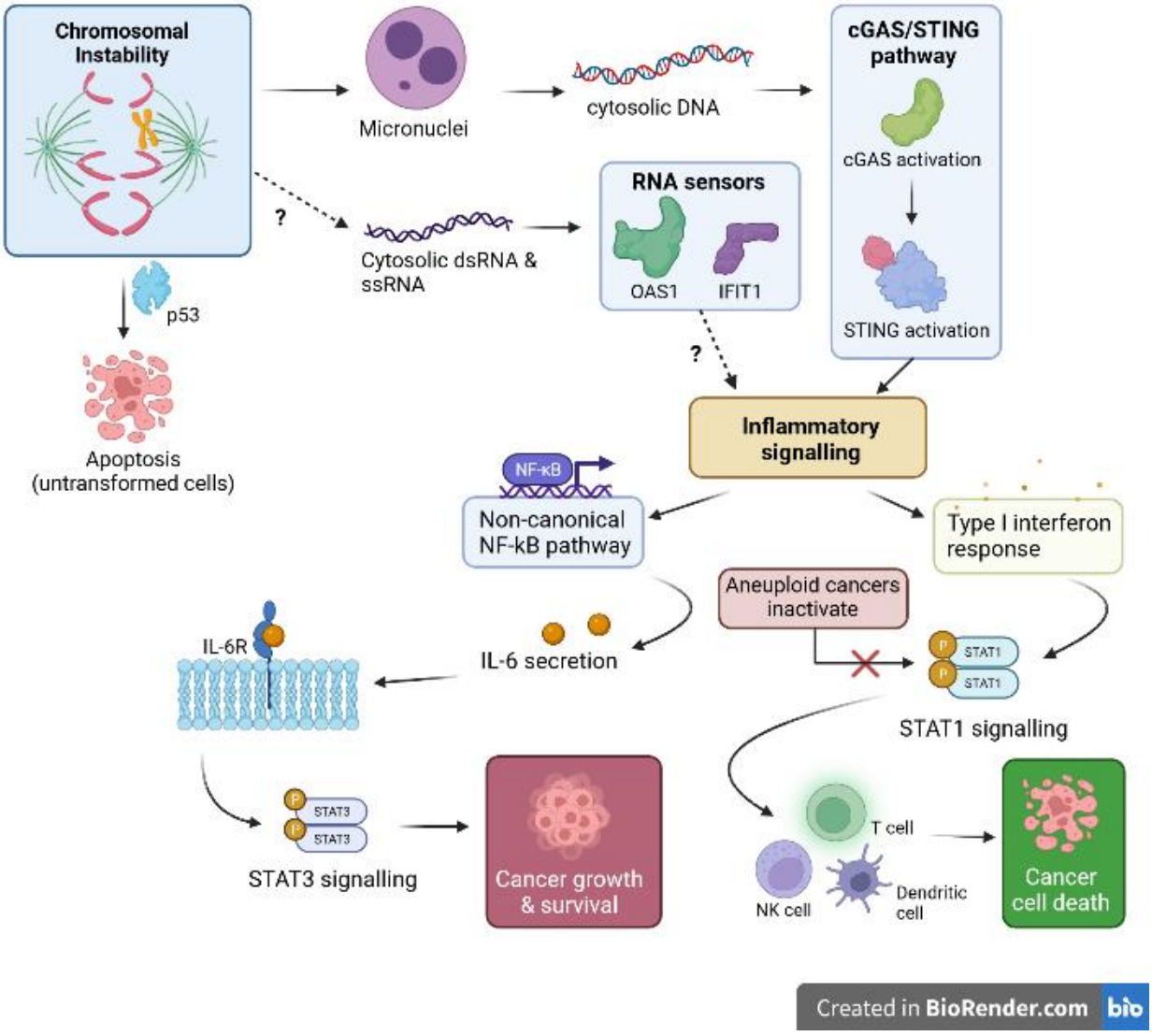

Figure 1: Schematic pathway in which CIN leads to cGAS/STING activation and subsequent inflammatory signalling involving STAT1 and STAT3 [created with BioRender.com and adapted from Hong et al., 2022]
cGAS/STING activates the type I interferon response, which leads to the production of inflammatory cytokines, STAT1 signalling, immune cell recruitment and subsequent killing of the cancer cell [Chen et al., 2022]. Simultaneously, the non-canonical NF-kB pathway leads to secretion of IL-6, which binds to the IL-6 receptor (IL-6R), ultimately leading to activation of STAT3 and cell survival [Hong et al., 2022]. RNA sensors, like OAS1 and IFIT1, might also be activated following CIN and lead to inflammatory signalling.

The broader goal of the research is to better understand how inflammatory signalling, following CIN, contributes to cell survival and to elucidate the mechanisms that aneuploid cancer cells exploit to escape immune recognition after this inflammatory response. In our project, the first steps will be taken. Knockout cell lines will be made for STAT1 and p53, which are confirmed to be important in the response against aneuploidy [Schubert et al., 2021]. Secondly, knockouts of IFIT1 and OAS1 will be made, which encode proteins that may be involved in the CIN-caused inflammatory response, based on bioinformatical analysis. Interferon-induced protein with tetratricopeptide repeats 1 (IFIT1) is known as a detector of viral ssRNA, but seems to play a role in cancer progression too [Abbas et al., 2013; Pidugu et al., 2019]. Secondly, 2'-5'-oligoadenylate synthetase 1 (OAS1) is an interferon-induced enzyme and dsRNA sensor, which plays a vital role in the innate immune response against viruses [Wickenhagen et al., 2021]. Interestingly, OAS1 is involved in drug resistance of tumour cells, and also seems to be a possible prognostic marker for certain cancer types [Che et al., 2021; Zhang & Yu, 2020].

In our project, HEK293 cells will be targeted with sgRNAs specific to the four genes mentioned above, followed by CRISPR-Cas9 knockout. HEK293 are chosen, as they are often used in CRISPR/Cas systems, are easy to grow and amenable to transfection [Cheng et al., 2013; Tan et al., 2021]. CIN can be induced in these HEK293 cells so that KO cells with and without CIN can be compared. CRISPR-Cas9 is often used to inactivate genes and consists of two main components: a single guide RNA (sgRNA) and Cas9 nuclease protein. The sgRNA-Cas9 complex will target and cut a specific DNA sequence, which leads to gene inactivation, as will be described more precisely in the method section [Sun et al., 2016.]. Knockout cell lines can contribute to research about the inflammatory pathway induced by CIN.

Firstly, sgRNAs will be designed and cloned into pX-459 V2.0 (Cas9-2A-Puro) vectors. Secondly, it will be assessed whether the sgRNAs are cloned correctly into vectors using Sanger sequencing. Subsequently, these vectors will be transfected into HEK293 cells. Lastly, PCR and western blot will assess whether the knockouts were successful. The protein level of STAT1 was not decreased, while p53 showed a slight reduction. PCR and sequencing of the p53 gene showed no mutations at the sgRNA-Cas9 cutting site. In conclusion, the knockout of STAT1 and p53 in HEK293 cells seems unsuccessful.

Materials and Methods

The CRISPR-Cas9 system for gene inactivation

Knockouts were generated using the CRISPR-Cas9 technology. As described, the system consists of two components: a sgRNA and Cas9 protein. The sgRNA is a non-coding RNA of about 20 bases that leads the Cas9 endonuclease to a specific DNA sequence [Sun et al., 2016]. There, a double-strand break will be made by Cas9, leading to non-homologous end joining (NHEJ) of the DNA. Since NHEJ is error-prone, it can lead to random insertions and deletions, possibly resulting in frameshift mutations [Wan et al., 2021]. Therefore, targeting specific exon sequences with the sgRNA-Cas9 complex can lead to gene knockout.

Guide RNA and primer design for OAS1 & IFIT1

Guide RNAs targeting the human OAS1 and IFIT1 gene were designed by in silico cloning using CRISPR design in Benchling. Guide RNAs were chosen based on their inclusion of all isoforms of the OAS1 and IFIT1 protein. For the BbsI restriction site oligos were designed with a 5'-CACC (forward) and 5'-AAAC (reverse) overhang. The following guide RNAs were chosen for OAS1: gRNA1 targeting exon 1 (5'-CTTGGACACACACACAGGGT-3'), gRNA2 targeting exon 1 (5'-TGGCATGGTTGATTTGCATG-3') and gRNA3 targeting exon 2 (5'-GTACGAAGCTGAGCGCACGG-3'). The following guide RNAs were chosen for IFIT1: gRNA1 targeting exon 2 (5'-TCGAAAGACATAGGTCTGTG-3') and gRNA2 targeting exon 2 (5'-GTGTCCAGAAATAGACTGTG-3'). Primers were designed surrounding the sgRNA regions to later validate the knockout in HEK293 cells. Guide RNAs and primers were ordered from the IDT company. Guide RNAs for p53 and STAT1 were readily available and contained the following sequences: 5'-GAAGGGACAGAAGATGACAG-3' and 5'-GTCCGCAACTATAGTGAACCT-3', respectively.

Cloning of sgRNAs in vectors & growing *E. coli* containing the vector

Cloning was performed as described in Nature Protocols [Ran et al., 2013], in short: (1) phosphorylation and annealing of the oligos, (2) the digestion-ligation reaction, (3) treatment of the ligation reaction with PlasmidSafe exonuclease and (4) transformation in bacteria. The backbone vector used is pX459 V2.0 (WT-2A-Puro V2.0 62988 from Addgene). The bacteria used were *Escherichia coli* (*E. coli*) strain DH5α. The bacteria were transformed with the vector using the heat-shock method at 42 °C. The transformed bacteria were plated on LB + agar plates with ampicillin (Amp) (100 ng/µL) and incubated overnight at 37 °C. Ampicillin resistance is encoded in the vector so that bacteria containing the vector are selected. Multiple colonies (6 for both STAT1 and p53; 4 for both OAS1 and IFIT1 per sgRNA) were selected and grown in 3 mL LB medium with ampicillin (100 ng/µL) for 24 hours at 37 °C in the shaking incubator. glycerol stocks of all clones were prepared and stored in -80 °C freezer. Thermo Scientific™ GeneJET Plasmid Miniprep Kit was used to isolate the plasmid DNA of the remaining cell cultures; the purification protocol for high-copy number plasmids was applied. DNA concentrations were measured by NanoDrop and plasmids were sent to Eurofins for Sanger sequencing with primer (U6 fwd: 5'-GAGGGCCTATTTCCCATGATTCC-3'), to check which clones had inserted the correct sgRNA. DNA sequences were analysed and aligned with plasmid pX459 V2.0+sgRNA.

The following steps were only performed for sgRNAs of p53 and STAT1. One clone was chosen per sgRNA based on the alignment. A starter culture was created from the glycerol stock. The starter culture was 1000x diluted in 100 mL LB + Amp and incubated in the shaking incubator at 37 °C for 24 hours. NucleoBond Xtra Midi kit for transfection-grade plasmid DNA was used to isolate plasmids from the p53 and STAT1 sgRNA cultures. The pellet containing the purified plasmids was resuspended with 250 µL TE buffer and stored at 4 °C. DNA concentration was measured using NanoDrop.

Cell culture

Human embryonic kidney (HEK293) cells were thawed and seeded in a 25cm2 culture flask and cultured in 5 mL Dulbecco's modified Eagle medium (DMEM) supplemented with 10% Fetal Bovine Serum (FBS) and 100U/mL Penicillin-Streptomycin. The HEK293 cells were grown in a 37 °C incubator for two days. For cell passage, first, the medium was discarded. Next, the cells were washed with Phosphate Buffered Saline (PBS) and subsequently discarded. After 0.25% trypsin was added to the adherent cells, the cells were incubated for 5 min at 37°C. After incubation, 5 mL DMEM medium was added to the cells, and vigorously pipetted and diluted into three 75 cm2 culture flasks. For optimal growth, the cells got fresh medium after 4 days.

Transfection

One day before transfection, cells were plated on 6-well plates. For this, the medium was discarded, and the cells were washed with 10 mL PBS and treated with 3 mL 0.25% trypsin. After incubation of 5 min at 37 °C, 4 mL medium was added to each flask, cells were collected and centrifuged for 5 mins at 300x g at 22 °C, after which the medium was discarded and a cell pellet remained. The pellet was resuspended in 5 mL fresh DMEM. 15 µL medium containing the cells was put in a 1 mL Eppendorf tube, to which 15 µL Trypan Blue was added. With an automatic cell counter, the cells were counted. 1 mL contained 6.5 x 106 cells. Approximately 300,000 cells were plated on each well of a 6-well plate in 2 mL medium. The plates were incubated in a 37 °C incubator for a day.

The FuGENE® HD Transfection Reagent protocol was prepared by mixing 9 µL FuGENE® reagent and 3 µg of each plasmid DNA (ratio FuGENE:DNA = 3 µL:1 µg), Opti-MEM was added to reach a total volume of 200 µL. The reaction was incubated for 15 minutes at room temperature and after which it was distributed to the 6-well plates. The plasmids used for transfection contained sgRNAs targeting p53 or STAT1 and three controls. The positive control was the empty pX459-puro-Cas9 plasmid, without sgRNA. The pX458-GFP (green fluorescent protein) plasmid was used to visualize transfection efficiency. The negative control was cells containing no plasmids, which is a control for puromycin resistance.

Puromycin selection

Puromycin selection was started 72 hours after transfection. HEK293 cells that were transfected on 6-well plates, were treated with 2 mL DMEM medium with puromycin (2 µg/mL) (p53, STAT1, pX459 and negative control) or 2 mL DMEM medium (pX458).
The plates were incubated at 37 °C. After 24 hours, the medium was refreshed.

Validation of the STAT1 and p53 knockout using PCR and western blot

The cells not used for puromycin selection were used for the validation of KO of STAT1 and p53. Cells were harvested by vigorously washing with PBS and split in half for DNA and protein extraction. The tubes were centrifuged for 5 minutes at 300x g at 22 °C. The PBS was discarded and the tubes were stored at -20 °C. For the PCR of the p53 gene, the cell pellet containing the STAT1, p53, pX459 plasmids and the negative control, were used. The DNA was isolated from the cells using the DNeasy® Blood & Tissue Kit and eluted in 100 µL AE buffer. To determine the DNA concentration, the NanoDrop was used. The samples were diluted to 50 ng/µL. 50 µL PCR mix containing p53 forward and p53 reverse primer (0.5 µM) and 100 ng plasmid DNA (50 ng/µL) was prepared for each sample. Either, p53, STAT1, pX459 or the negative control isolated DNA. Water was used as a negative control for PCR. PCR bands at 740 bp (p53) for the samples p53 and STAT1 were cut out of the agarose gel. DNA was isolated from the agarose gel with the Zymo DNA clean and concentrator kit and sent to IDT company for sequencing.

For the western blot, the general protocol for western blotting from BioRad was used. The cell pellets (p53, STAT1, pX458, pX459 and negative control) were resuspended in 100 µL ELB buffer, to which 1/50 diluted protease inhibitor was added. The cells were centrifuged in a tabletop centrifuge at 4 °C for 5 min at 500 x g, after which the cell debris was discarded. The western blot samples were mixed 5:1 with sample buffer (SDS + DTT), after which they were heated for 5 minutes at 96 °C. Subsequently, samples were run on an SDS-Page gel on a running buffer for one hour at 100 V followed by an hour at 200 V. The proteins were transferred onto polyvinylidene difluoride (PVDF) membranes followed by 5-minute incubation at room temperature with a blocking buffer. The PVDF membranes were incubated overnight with anti-p53 (SC-126, mouse host, diluted 1:500 in blocking buffer), anti-Actin 4970 (rabbit host, 1:5000 in blocking buffer), anti-STAT1 (9772S, rabbit host, 1:1000 in blocking buffer) and anti-Actin 3700 (mouse host, 1:5000 in blocking buffer) at 4 °C on a roller. The membranes were washed three times with TBS-Tween (TBS-T) and incubated with secondary antibodies, anti-rabbit-IR800 (αR, 1:10000 in blocking buffer) and anti-mouse-IR700 (αM, 1:10000), for one hour at room temperature with gentle agitation followed by three washes with TBS-T and one final one with TBS. In the western blot, the colour tags for αR and αM were green and red, respectively. The blots were imaged and quantified with the Odyssey system.

Results

Validation of sgRNA incorporation in plasmids

To create knockouts, sgRNAs for p53, STAT1, IFIT1, and OAS1 were cloned into backbone vectors. The resulting sequences were compared to plasmid templates to validate whether the sgRNAs were indeed taken up by the plasmids. In Benchling the plasmid sequences were aligned to the corresponding complementing templates (see figure 1A, for example).
For each sgRNA design, there was a plasmid clone that had correctly incorporated the sgRNAs, because the DNA sequence of the template and the cloned vectors were identical at the sgRNA site (figure 1B-H). Therefore we can conclude that for all 4 genes plasmid cloning was successful.

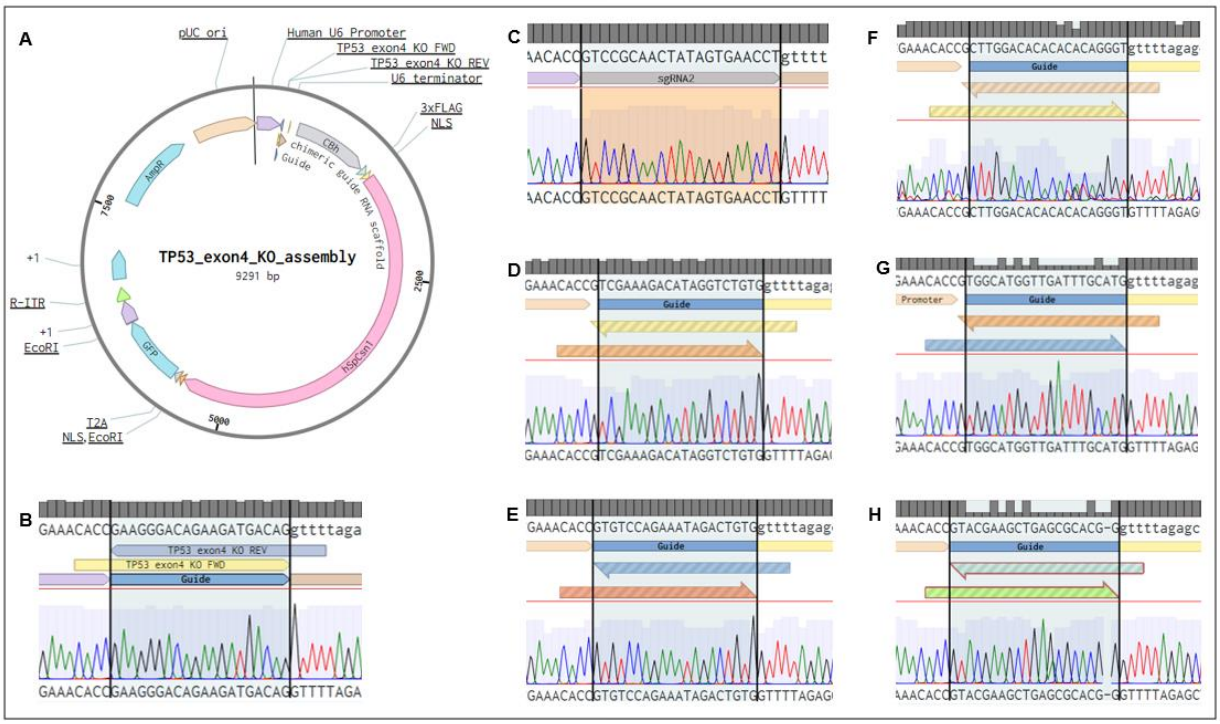

Figure 2: Benchling alignment validation for sgRNA in plasmids

A. Vector map of pX459_V2.0_p53

B. - H. Sequence alignment of sgRNA in exon 4 of p53 (B), exon 10 of STAT1 (C), exon 2 of IFIT1 #1 (D), exon 2 of IFIT 1 #2 (E), exon 1 of OAS1 #1 (F), exon 1 of OAS1 #2 (G), and exon 2 of OAS1 (H). The DNA sequence on top is the template sequence and the bottom DNA sequence is the sequence of the plasmid with the incorporated sgRNA. Alignments created in Benchling.

HEK293 cells were chosen as target cells

To create knockout cell lines, we used HEK293 cells. HEK293 cells are derived from the primary cultures of Human Embryonic Kidney cells by transformation with sheared fragments of adenovirus 5 DNA [Shaw et al., 2002]. HEK293 cells are often used in research using CRISPR/Cas9 for knocking out genes [Ebina et al., 2013; Chen et al., 2013; Cheng et al., 2013]. According to cytogenetic analysis, the 293 cell line is pseudo-triploid [Bylund et al., 2004]. The average chromosome number in HEK293 cells is 64, in 30% of the cells, with higher ploidy occurring in 4.2% of the cells. They have three copies of the X chromosome, and a 4 kbp fragment of AD5 incorporated into chromosome 19, which display cytogenetic instability [Synthego, n.d.].

Transfection of HEK293 cells with pX458-GFP, pX459-Puro-p53 and pX459-Puro-STAT1

HEK293 cells were transfected with pX459 vectors containing sgRNAs for STAT1 or p53. Positive control cells were transfected with pX458-GFP vectors. Negative control cells were transfected with the empty pX459 vector. A second negative control consisted of cells transfected with saline (no vector). Positive control cells were visualized by microscopy (see figure 3A-F). The majority of these cells were positive for GFP expression, as visible in an overlay of bright-field and fluorescence microscopy (figure 3C and 3F). As most of the positive control cells seemed to be successfully transfected, no puromycin selection was done before knockout validation (western blot and PCR) of HEK293 cells transfected with vectors containing sgRNAs.

Puromycin selection was performed on the remaining part of the HEK293 cells transfected with pX459 vectors. Cells were incubated in DMEM with puromycin (2 µg/mL) for 24 hours at 37 °C, between 72 and 96 hours after transfection. Microscopy showed that cells transfected with pX459 vectors were still adherent (figure 3G). Negative control cells without the pX459 vector had a round morphology and were largely detached from the culture flask (figure 3H). The cells were incubated in puromycin containing DMEM for more than 24 hours (after microscopy). At later time points, cells with the pX459 vector also detached from the culture flask and had a round morphology, indicating that they died.

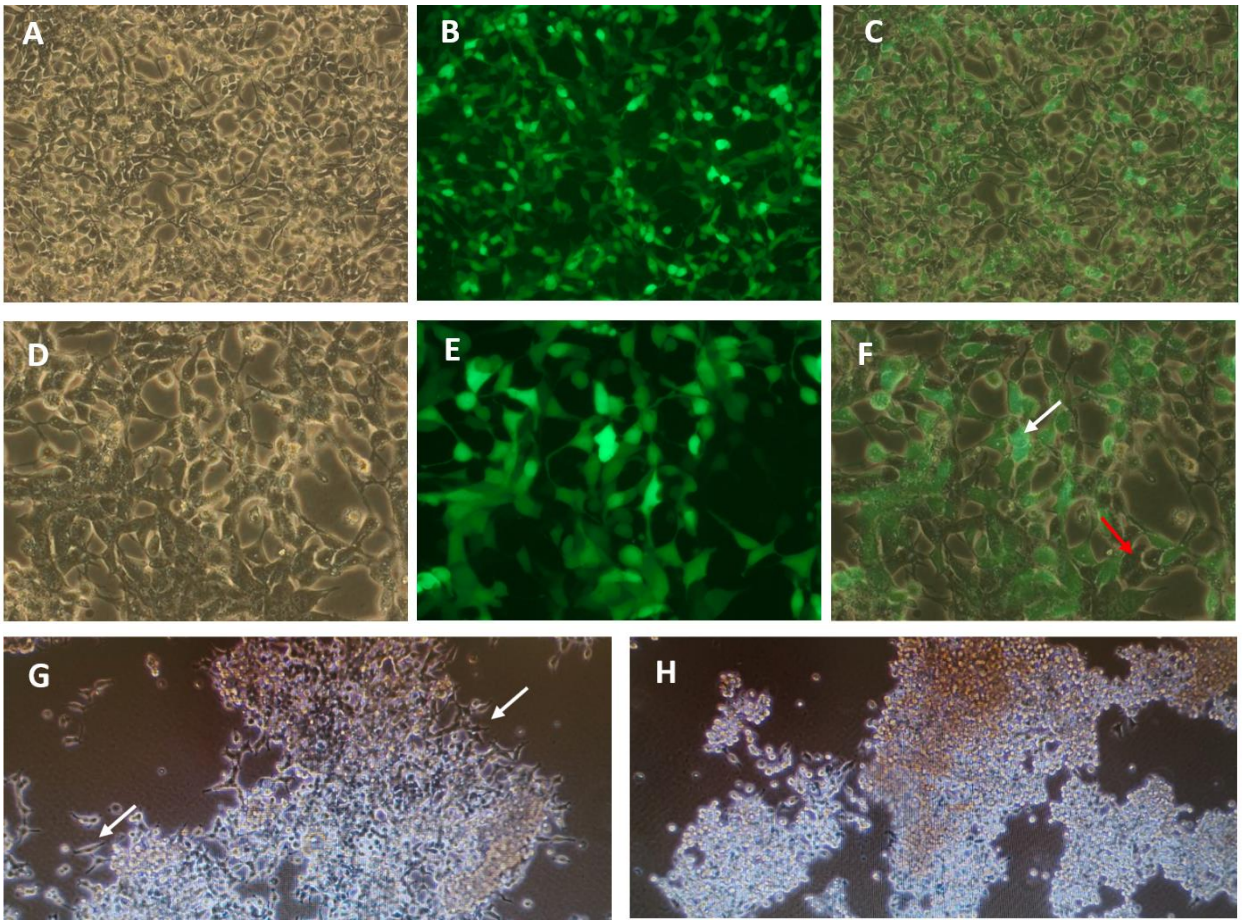

Figure 3: Transfection of HEK293 cells

A. Bright-field microscope picture of HEK293 cells 24 hours after transfection with the vector pX458, containing green-fluorescent protein (GFP). 40x magnification.
B. The same picture as (A) was visualized using fluorescent light, which visualizes GFP as green fluorescence.
C. Overlay of panel (A) and (B), showing positive and negative cells for the GFP vector.
D. Fluorescence microscopy picture of HEK293 cells that were transfected with the pX458-GFP vector. 100x magnification
E. The same picture as (D) using fluorescent light. GFP is visible as green fluorescence.
F. Overlay of panel (D) and (E), showing the cells that are positive and negative for the GFP vector. Examples of positive and negative cells are given by white and red arrows, respectively.
G. Microscopic image of HEK293 cells transfected with empty backbone vector pX459 V2.0 (WT-2A-Puro) after 24 hours of incubation in DMEM with puromycin (2 µg/mL). Cell cultures of HEK293 cells transfected with pX459, containing sgRNAs for STAT1 or p53, looked similar (not shown), 24 hours after incubation in DMEM with puromycin (2 µg/mL) at 37 °C. Puromycin selection was started 72 hours after transfection. Cell attachment is visible, indicated with white arrows.
H. Microscopic image of HEK293 cells treated with saline transfection reagent (negative control) after 24 hours of incubation in DMEM with puromycin (2 µg/mL) at 37°C. The vast majority of cells had detached from the culture flask and had a round morphology.

Validation of STAT1 and p53 KO HEK293 cells

p53 and STAT1 KO HEK293 cells were generated with the CRISPR/Cas9 technology. sgRNAs for p53 and STAT1 were cloned into pX459 V2.0 vectors, which were transfected into the HEK293 cells. The sgRNA-Cas9 complex would cause a double-stranded break. Non-Homologous End-Joining (NHEJ) would lead to insertions or deletions in exon 4 for p53 and in exon 10 for STAT1, theoretically leading to a frameshift 2 out of 3 times. PCR and sequencing were used to validate the mutation in the p53 gene. HEK293 samples, containing the p53 plasmid and 4 controls were separated on fragment size, using p53 primers (see figure 4A). This figure shows that each sample, except water, contained the p53 fragment, but between 100 and 500 bp non-specific binding occurred in all samples, except the water lane.

The p53 PCR band was cut out of the agarose gel for cells transfected with sgRNAs for p53 or STAT1 (negative control). The p53 gene was isolated from these samples with Zymo DNA clean and concentrator kit and sent for Sanger sequencing. Alignment of the sgRNA sequence with a wildtype (wt) p53 template, showed that there were no mutations in the sgRNA sequence of the STAT1 sample, as expected (see figure 4B). There were also no mutations in the sgRNA sequence of the p53 sample (figure 4B), thereby indicating that the KOs were probably not successful. Interestingly, the sequence preceding the sgRNA contained a lot of mismatches in both the cells transfected with sgRNAs for p53 and the negative control. This indicates that the HEK293 cells probably already had mutations in the p53 gene.

Furthermore, KOs of STAT1 and p53 HEK293 cells were validated by western blot. The absence or decrease in protein levels of p53 and STAT1 indicates a KO (figure 4C-D). Protein level was quantified with the ratio of intensity STAT1/Actin and p53/Actin (figure 4C-F). The Actin 3700 band was used for both the p53 and STAT1 quantification, as the Actin 4970 was not visible. The western blot showed that there was no decrease in STAT1 protein expression (figure 4E), which suggests that there were probably no STAT1 KOs HEK293 cells. However, the p53 protein level was slightly decreased in cells targeted for p53 KO (figure 4F). Remarkably, a non-specific band was detected at around 100 kDa in all lanes (figure 4C and 4D). In addition, there was a green band visible at approximately 50 kDa in figure 4D.

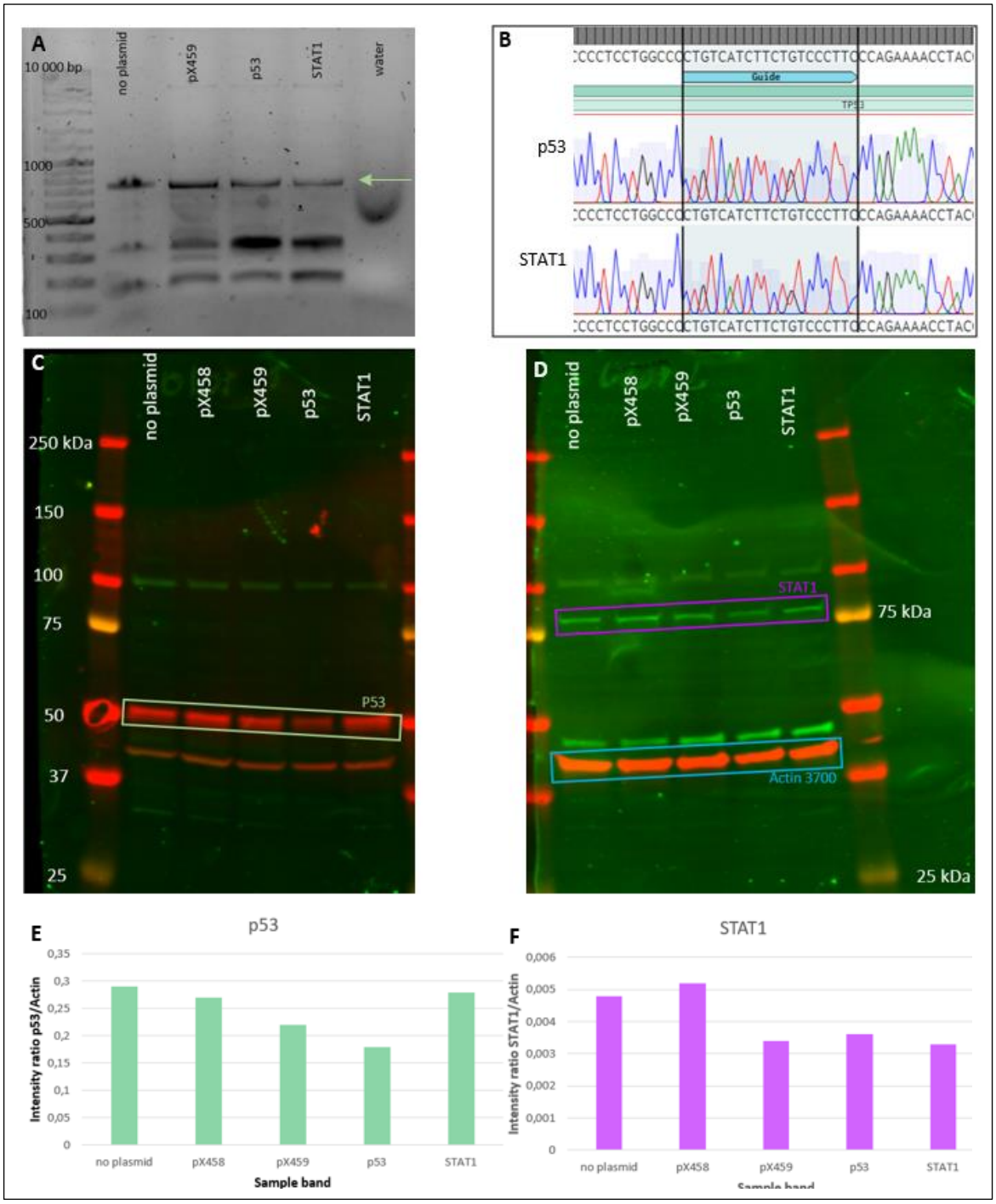

Figure 4: PCR and western blot in transfected HEK293 cells

A. PCR of the p53 gene in HEK293 cells, 72 hours after transfection with pX459 with sgRNA for p53. The presence of the p53 gene was validated for the cells targeted for p53 KO and control cells, as seen in the bands at 740 bp (green arrow). The negative control ("water") did not contain a DNA sample and correspondingly showed no p53 band.

B. Sanger sequencing results of p53 editing in STAT1 and p53 targeted cells, compared to the wt p53 gene template.

C. Western blot analysis of p53 expression in HEK293 genome-edited cell lines with, from right to left, no DNA control, pX458-GFP plasmid, pX459 plasmid, KO p53 and KO STAT1.

D. Western blot analysis of STAT1 expression in HEK293 genome-edited cell lines.

E. Quantification of the p53 protein levels measured in the western blot (C). Expression levels of p53 were compared to actin expression levels.

F. Quantification of the STAT1 protein levels measured in the western blot (D). Expression levels of STAT1 were compared to actin expression levels.

Discussion

The goal of this research was to create knockout HEK293 cells for the genes OAS1, IFIT1, STAT1, and p53. To achieve this, sgRNAs were created and cloned into vectors, which were transfected into the target cells. Notably, only vectors containing sgRNASs for STAT1 and p53 were used for transfection. Western blot and PCR analyses were performed to validate the knockout of these genes. No reduction in STAT1 protein quantity was found, while there was a slight reduction in p53 level. Sanger sequencing following a PCR of the p53 gene revealed no mutations at the sgRNA-Cas9 cutting site.

First of all, even when sgRNA was incorporated correctly into the CRISPR-Cas vector, the efficiency of the sgRNA-Cas9 complex is unknown. As a result, it is unsure whether the sgRNA-Cas9 cuts the targeted DNA sequence and whether gene inactivation can be achieved. HEK293 cells may therefore be puromycin resistant, but at the same time express a sgRNA-Cas9 complex that is non-functional. Consequently, these cells can grow in a puromycin-containing medium, while they do not have a knockout of the target genes.

Additionally, a full gene knockout is only achieved when all alleles of the cell are inactivated. HEK293 cells were found to be near-triploid, as they had between 62 and 70 chromosomes per cell [Bylund et al., 2004]. According to karyotyping, the HEK293 has three chromosomes 17, on which the p53 gene is located [Bylund et al., 2004; McBride et al., 1986]. An additional chromosome that contains the target gene, makes it harder to achieve a full knockout. However, HEK293 cells seem to be suitable for KO models, as they are still used in recent research [Abaandou et al., 2021].

In general, transfection leads to a polyclonal cell culture. This happens because the sgRNA-Cas9 complex makes a double-strand break in the DNA, leading to NHEJ and random insertions and deletions (indels). However, NHEJ will create different indels in all cells, and only a part of these mutations will be out-of-frame and thereby inactivate the gene. This means that not all cells have the knockout, and those who do can have a plethora of mutations. Preferably, a stable KO cell line with a specific mutation will be selected and cultured for further research [Giuliano et al., 2019]. Unfortunately, this was not done in our research because of time restrictions.

Furthermore, FuGENE is a transient transfection agent, meaning that plasmid DNA is inserted into the transfected cell, but it is not incorporated into its genome [Marucci et al., 2011]. Consequently, plasmids will be gradually lost, as not all daughter cells will receive the plasmid. Conversely, there may be cells that have a knockout, but their daughter cells may lose the vector and thereby puromycin resistance. Thus, puromycin selection may kill successful KO cells. Western blot and PCR were performed 72 hours after transfection, implying that the vector containing sgRNAs may have already diluted. Lentiviral vectors can be favoured, as they can integrate permanently into the genome [Mao et al., 2015]. However, activation of the sgRNA-Cas9 complex is only needed once for a KO, so persistent Cas9 protein activation in the target cell is unwanted and can be deleterious.

Moreover, cells may not have been puromycin resistant anymore, as puromycin selection was performed between 72 and 96 hours after transfection, and plasmids only survive up to 4 days in mammalian cells [Creative Biogene Technology, n.d.]. Maintaining the puromycin selection for longer means HEK293 may die, although the cells were transfected successfully in the first place. We speculate that this was the case, considering all transfected HEK293 cells (transfected with empty pX459 vector, pX459 containing sgRNA for p53 and pX459 containing sgRNA for STAT1) had detached and died after puromycin selection between 24-96 hours. Furthermore, culture conditions were not optimal, as the culture flasks were full and the medium was exhausted, which can be another reason for cell death.

In addition, confounding results may have been found in the western blot, as there was no puromycin selection performed on the cells used for this validation step. Our assumption that the transfections with the vectors targeting p53 and STAT1 had been as successful as the GFP-encoding vector, may have been wrong. Moreover, non-specific binding occurred in multiple bands on the western blot, while the Actin 4970 band was lacking. The latter impaired quantification of the p53 protein, as the Actin 3700 had to be used for this. The green band at 50 kDa (see figure 4D) may have been an additional signal of the STAT1 antibody (9772S) [Cell Signaling Technology, n.d.].

Unfortunately, primers for the STAT1 gene were unavailable, and therefore PCR and Sanger sequencing could not be performed. In Sanger sequencing of the p53 gene, no mutations were found at the sgRNA site in cells targeted for p53 KO. However, many mutations occurred upstream of this sequence, also in the negative control cells. There's a possibility that our HEK293 cells had mutations in the p53 gene in the first place, although the HEK293 cell line normally possesses a wt p53 gene [Sun et al., 2010]. Furthermore, we speculate that these mutations may have impaired primer binding and possibly led to malfunctioning of the Sanger sequencing.

All in all, sgRNAs for all four genes were cloned correctly into the backbone vector. Our research was limited by time constraints, which resulted in the fact that the transfection was not performed with vectors targeting OAS1 and IFIT1. Suboptimal culturing conditions may have impacted the transfection efficiency and puromycin selection. Although the GFP-encoding vector was expressed highly in transfected cells, the other transfections and KOs seem to have been unsuccessful, as shown by western blot, PCR and Sanger sequencing. The reliability of these validation steps is impacted by the fact that puromycin selection was not performed beforehand. Due to the lack of sequencing data on the STAT1 gene, it also cannot be guaranteed that the KO was without success.

In conclusion, the objective to make a knockout of STAT1 and p53 in HEK293 appears to not be realised. For efficient vector expression, it is important to take enough time, although plasmid dilution should be avoided. We recommend using lentiviral vectors to avoid difficulties with transient transfection agents. Moreover, we suggest following a different protocol for puromycin selection and cell culturing. Furthermore, knockouts may be laborious to achieve in near-triploid HEK293 cells, especially when the chromosome encoding the target gene is multiplied. Therefore, we suggest using a different cell line to create p53 KOs. In addition, future work should involve the generation of OAS1 and IFIT1 KO cell lines. These would be advantageous for research about the inflammatory pathway induced by CIN.

References

Abaandou, L., Sharma, A. K., & Shiloach, J. (2021). Knockout of the caspase 8-associated protein 2 gene improves recombinant protein expression in HEK293 cells through up-regulation of the cyclin-dependent kinase inhibitor 2A gene. *Biotechnology and bioengineering*, **118**(1), 186–198.

Abbas, Y. M., Pichlmair, A., Górna, M. W., Superti-Furga, G., & Nagar, B. (2013). Structural basis for viral 5'-PPP-RNA recognition by human IFIT proteins. *Nature*, **494**(7435), 60–64.

Bakhoum, S. F., Ngo, B., Laughney, A. M., Cavallo, J. A., Murphy, C. J., Ly, P., Shah, P., Sriram, R. K., Watkins, T., Taunk, N. K., Duran, M., Pauli, C., Shaw, C., Chadalavada, K., Rajasekhar, V. K., Genovese, G., Venkatesan, S., Birkbak, N. J., McGranahan, N., Lundquist, M., … Cantley, L. C. (2018). Chromosomal instability drives metastasis through a cytosolic DNA response. *Nature,* **553**(7689), 467–472.

Ben-David, U., & Amon, A. (2020). Context is everything: aneuploidy in cancer. *Nature reviews. Genetics*, **21**(1), 44–62.

Bylund, L., Kytölä, S., Lui, W. O., Larsson, C., & Weber, G. (2004). Analysis of the cytogenetic stability of the human embryonal kidney cell line 293 by cytogenetic and STR profiling approaches. *Cytogenetic and genome research*, **106**(1), 28–32.

Cell Signaling Technology. (n.d.). *Stat1 Antibody #9172*. Retrieved June 7, 2022, from https://www.cellsignal.com/products/primary-antibodies/stat1-antibody/9172

Che, L., Yang, H., Wang, D., & Liu, S. (2021). Corylin sensitizes breast cancer cells to overcome tamoxifen resistance by regulating OAS1/miR-22-3p/SIRT1 axis. *Acta biochimica Polonica*, **68**(4), 757–764.

Chen, B., Gilbert, L. A., Cimini, B. A., Schnitzbauer, J., Zhang, W., Li, G. W., Park, J., Blackburn, E. H., Weissman, J. S., Qi, L. S., & Huang, B. (2013). Dynamic imaging of genomic loci in living human cells by an optimized CRISPR/Cas system. *Cell*, **155**(7), 1479–1491.

Chen, M., Linstra, R., & van Vugt, M. (2022). Genomic instability, inflammatory signaling and response to cancer immunotherapy. *Biochimica et biophysica acta. Reviews on cancer*, **1877**(1), 188661.

Cheng, A. W., Wang, H., Yang, H., Shi, L., Katz, Y., Theunissen, T. W., Rangarajan, S., Shivalila, C. S., Dadon, D. B., & Jaenisch, R. (2013). Multiplexed activation of endogenous genes by CRISPR-on, an RNA-guided transcriptional activator system. *Cell research*, **23**(10), 1163–1171.

Creative Biogene Biotechnology. (n.d.). *Transient Transfection Protocol.* Creative Biogene. Retrieved June 6, 2022, from https://www.creative-biogene.com/support/Transient-transfection-protocol.html

Diamond, M. S., Kinder, M., Matsushita, H., Mashayekhi, M., Dunn, G. P., Archambault, J. M., Lee, H., Arthur, C. D., White, J. M., Kalinke, U., Murphy, K. M., & Schreiber, R. D. (2011). Type I interferon is selectively required by dendritic cells for immune rejection of tumors. *The Journal of experimental medicine*, **208**(10), 1989–2003.

Duijf, P. H. G., Schultz, N., & Benezra, R. (2013). Cancer cells preferentially lose small chromosomes. *International journal of cancer*, **132**(10), 2316–2326.

Ebina, H., Misawa, N., Kanemura, Y., & Koyanagi, Y. (2013). Harnessing the CRISPR/Cas9 system to disrupt latent HIV-1 provirus. *Scientific reports*, **3**, 2510.

Giuliano, C. J., Lin, A., Girish, V., & Sheltzer, J. M. (2019). Generating Single Cell-Derived Knockout Clones in Mammalian Cells with CRISPR/Cas9. *Current protocols in molecular biology*, **128**(1), e100.

Glück, S., Guey, B., Gulen, M. F., Wolter, K., Kang, T. W., Schmacke, N. A., Bridgeman, A., Rehwinkel, J., Zender, L., & Ablasser, A. (2017). Innate immune sensing of cytosolic chromatin fragments through cGAS promotes senescence. *Nature cell biology*, **19**(9), 1061–1070.

Gordon, D. J., Resio, B., & Pellman, D. (2012). Causes and consequences of aneuploidy in cancer. *Nature reviews. Genetics*, **13**(3), 189–203.

Hatch, E. M., Fischer, A. H., Deerinck, T. J., & Hetzer, M. W. (2013). Catastrophic nuclear envelope collapse in cancer cell micronuclei. *Cell,* **154**(1), 47–60.

Hong, C., Schubert, M, Tijhuis, A.E., Requesens, M., Roorda, M., van den Brink, A., Ruiz, L.A., Bakker, P.L., van der Sluis, T., Pieters, W., Chen, M., Wardenaar, R., van der Vegt, B., Spierings, D.C.J., de Bruyn, M., van Vugt, M.A.T.M., Foijer, F. (2022). Inhibition of IL6 signalling as a therapeutic strategy to eradicate cancer cells with chromosomal instability. *Unpublished.*

Kadioglu, O., Saeed, M., Mahmoud, N., Azawi, S., Mrasek, K., Liehr, T., & Efferth, T. (2021). Identification of potential novel drug resistance mechanisms by genomic and transcriptomic profiling of colon cancer cells with p53 deletion. *Archives of toxicology*, **95**(3), 959–974.

Mackenzie, K. J., Carroll, P., Martin, C. A., Murina, O., Fluteau, A., Simpson, D. J., Olova, N., Sutcliffe, H., Rainger, J. K., Leitch, A., Osborn, R. T., Wheeler, A. P., Nowotny, M., Gilbert, N., Chandra, T., Reijns, M., & Jackson, A. P. (2017). cGAS surveillance of micronuclei links genome instability to innate immunity. *Nature*, **548**(7668), 461–465.

Mao, Y., Yan, R., Li, A., Zhang, Y., Li, J., Du, H., Chen, B., Wei, W., Zhang, Y., Sumners, C., Zheng, H., & Li, H. (2015). Lentiviral Vectors Mediate Long-Term and High Efficiency Transgene Expression in HEK 293T cells. *International journal of medical sciences*, **12**(5), 407–415.

Marucci, G., Lammi, C., Buccioni, M., Dal Ben, D., Lambertucci, C., Amantini, C., Santoni, G., Kandhavelu, M., Abbracchio, M. P., Lecca, D., Volpini, R., & Cristalli, G. (2011). Comparison and optimization of transient transfection methods at human astrocytoma cell line 1321N1. *Analytical biochemistry*, **414**(2), 300–302.

McBride, O. W., Merry, D., & Givol, D. (1986). The gene for human p53 cellular tumor antigen is located on chromosome 17 short arm (17p13). *Proceedings of the National Academy of Sciences of the United States of America*, **83**(1), 130–134.

Musacchio A. (2015). The Molecular Biology of Spindle Assembly Checkpoint Signaling Dynamics. *Current biology : CB,* **25**(20), R1002–R1018.

Pidugu, V. K., Pidugu, H. B., Wu, M. M., Liu, C. J., & Lee, T. C. (2019). Emerging Functions of Human IFIT Proteins in Cancer. *Frontiers in molecular biosciences*, **6**, 148.

Ran, F. A., Hsu, P. D., Wright, J., Agarwala, V., Scott, D. A., & Zhang, F. (2013). Genome engineering using the CRISPR-Cas9 system. *Nature protocols*, **8**(11), 2281–2308.

Schubert, M., Hong, C., Jilderda, L.J., Requesens Rueda, M., Tijhuis, A.E., Simon, J.E., Bakker, P.L., Cooper, J.L., Damaskou, A., Wardenaar, R., Bakker, B., Gupta, S., van den Brink, A., Andrade Ruiz, L., Koster, M.H., Youssef, S.A., Luinenburg, D., Strong, A., Engleitner, T., Ponstingl, H., de Haan, G., de Bruin, A., Rad, R., Nijman, H.W., Medema, R.H., van Vugt, M.A.T.M., de Bruyn, M., Spierings, D.C.J., Colomé-Tatché, M., Vassiliou, G.S., Foijer, F. (2021). Cancer tolerance to chromosomal instability is driven by Stat1 inactivation in vivo. *bioRxiv* 471107\

Schukken, K. M., & Foijer, F. (2018). CIN and Aneuploidy: Different Concepts, Different Consequences. *BioEssays*, **40**(1), 1700147

Shaw, G., Morse, S., Ararat, M., & Graham, F. L. (2002). Preferential transformation of human neuronal cells by human adenoviruses and the origin of HEK 293 cells. *FASEB journal : official publication of the Federation of American Societies for Experimental Biology,* **16**(8), 869–871.

Sun, L., Lutz, B. M., & Tao, Y. X. (2016). The CRISPR/Cas9 system for gene editing and its potential application in pain research. *Translational perioperative and pain medicine*, **1**(3), 22–33

Sun, L., Shen, X., Liu, Y., Zhang, G., Wei, J., Zhang, H., Zhang, E., & Ma, F. (2010). The location of endogenous wild-type p53 protein in 293T and HEK293 cells expressing low-risk HPV-6E6 fusion protein with GFP. *Acta biochimica et biophysica Sinica*, **42**(3), 230–235.

Synthego. (n.d.). *HEK293 Cells: Background, Applications, Protocols, and More - A Guide to One of the Most Commonly Used Cell Lines*. Synthego. Retrieved May 29, 2022, from https://www.synthego.com/hek293

Tan, E., Chin, C., Lim, Z., & Ng, S. K. (2021). HEK293 Cell Line as a Platform to Produce Recombinant Proteins and Viral Vectors. *Frontiers in bioengineering and biotechnology,* **9**, 796991.

Thomas, P., & Smart, T. G. (2005). HEK293 cell line: a vehicle for the expression of recombinant proteins. *Journal of pharmacological and toxicological methods*, **51**(3), 187–200.

Wan, L., Wang, Z., Tang, M., Hong, D., Sun, Y., Ren, J., Zhang, N., Zeng, H. (2021). CRISPR-Cas9 gene editing for fruit and vegetable crops: strategies and prospects. *Horticulturae*, **7**, 193.

Wang, R. W., Viganò, S., Ben-David, U., Amon, A., & Santaguida, S. (2021). Aneuploid senescent cells activate NF-κB to promote their immune clearance by NK cells. *EMBO reports*, **22**(8), e52032.

Wickenhagen, A., Sugrue, E., Lytras, S., Kuchi, S., Noerenberg, M., Turnbull, M. L., Loney, C., Herder, V., Allan, J., Jarmson, I., Cameron-Ruiz, N., Varjak, M., Pinto, R. M., Lee, J. Y., Iselin, L., Palmalux, N., Stewart, D. G., Swingler, S., Greenwood, E., Crozier, T., … Wilson, S. J. (2021). A prenylated dsRNA sensor protects against severe COVID-19. *Science (New York, N.Y.)*, **374**(6567), eabj3624.

Zhang, Y., & Yu, C. (2020). Prognostic characterization of OAS1/OAS2/OAS3/OASL in breast cancer. *BMC cancer,* **20**(1), 575.